molecular pharmaceutics

Article

pubs.acs.org/molecularpharmaceutics

Microfibrous Solid Dispersions of Poorly Water-Soluble Drugs Produced via Centrifugal Spinning: Unexpected Dissolution Behavior on Recrystallization

Stefania Marano,[†] Susan A. Barker,[†] Bahijja T. Raimi-Abraham,[†,⊥] Shahrzad Missaghi,[‡] Ali Rajabi-Siahboomi,[‡] Abil E. Aliev,[§] and Duncan Q. M. Craig*[,†]

[†]School of Pharmacy, University College London, 29-39 Brunswick Square, London, WC1N 1AX, U.K.

[‡]Colorcon Inc., Global Headquarters, 275 Ruth Road, Harleysville, Pennsylvania 19438, United States

[§]Department of Chemistry, University College London, 20 Gordon Street, London, WC1H 0AJ, U.K.

ABSTRACT: Temperature-controlled, solvent-free centrifugal spinning may be used as a means of rapid production of amorphous solid dispersions in the form of drug-loaded sucrose microfibers. However, due to the high content of amorphous sucrose in the formulations, such microfibers may be highly hygroscopic and unstable on storage. In this study, we explore both the effects of water uptake of the microfibers and the consequences of deliberate recrystallization for the associated dissolution profiles. The stability of sucrose microfibers loaded with three selected BCS class II model drugs (itraconazole (ITZ), olanzapine (OLZ), and piroxicam (PRX)) was investigated under four different relative humidity conditions (11, 33, 53, and 75% RH) at 25 °C for 8 months, particularly focusing on the effect of the highest level of moisture (75% RH) on the morphology, size, drug distribution, physical state, and dissolution performance of microfibers. While all samples were stable at 11% RH, at 33% RH the ITZ−sucrose system showed greater resistance against devitrification compared to the OLZ− and PRX−sucrose systems. For all three samples, the freshly prepared microfibers showed enhanced dissolution and supersaturation compared to the drug alone and physical mixes; surprisingly, the dissolution advantage was largely maintained or even enhanced (in the case of ITZ) following the moisture-induced recrystallization under 75% RH. Therefore, this study suggests that the moisture-induced recrystallization process may result in considerable dissolution enhancement compared to the drug alone, while overcoming the physical stability risks associated with the amorphous state.

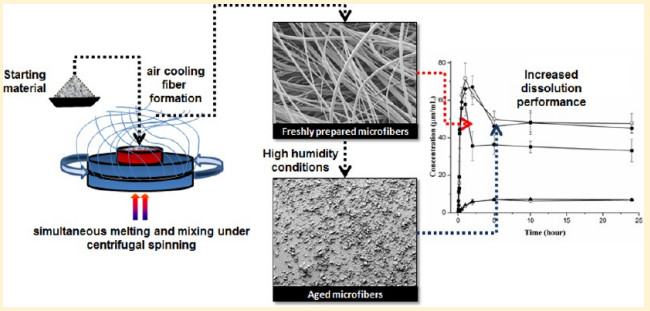

KEYWORDS: *centrifugal spinning, microfiber, amorphous, solid dispersion, crystallization, stability, poorly water-soluble drug, sucrose, supersaturation*

1. INTRODUCTION

The drug dissolution performance of BCS class II drugs is pivotal for attaining suitable oral absorption from the gastrointestinal tract, with associated therapeutic benefit. The incorporation of this class of drugs into fully amorphous solid dispersions represents a well-known and efficient technology to address low bioavailability resulting from poor water-solubility.[1] Amorphous materials lack the ordered molecular lattice of crystalline materials, hence the strength of intermolecular interactions is lower than in crystalline solids. The higher free energy state of amorphous drugs can lead to increased rates of dissolution and apparent solubility (often up to several orders of magnitude) and, in turn, higher bioavailability.[2−5]

Conventional methods for preparing amorphous solid dispersions include spray-drying, freeze-drying, and hot melt extrusion. These approaches may require specialized equipment, often associated with difficulties in scale-up.[6] Drug loaded microfibers represent a recent and potentially highly interesting approach to solid dispersion technology provided the issues associated with large scale production can be overcome. Our previous work explored the use of a solvent-free temperature-controlled centrifugal spinning process as an alternative technique for mass producing amorphous solid dispersions in the form of drug-loaded sucrose microfibers with enhanced dissolution performance.[7] This technique has promising large scale production capability and the microfibers produced showed significant dissolution improvements for the model drugs olanzapine (an antipsychotic drug) and piroxicam (a nonsteroidal anti-inflammatory) (both BCS class II) compared to the drugs alone or their physical mixtures with sucrose. This was mainly attributed to the amorphous nature of both the drug and the microfiber matrix, the solubilizing capability of sucrose, and the high surface area to volume ratio

Received: December 15, 2016
Revised: February 17, 2017
Accepted: March 15, 2017
Published: March 15, 2017

DOI: 10.1021/acs.molpharmaceut.6b01126
Mol. Pharmaceutics 2017, 14, 1666−1680

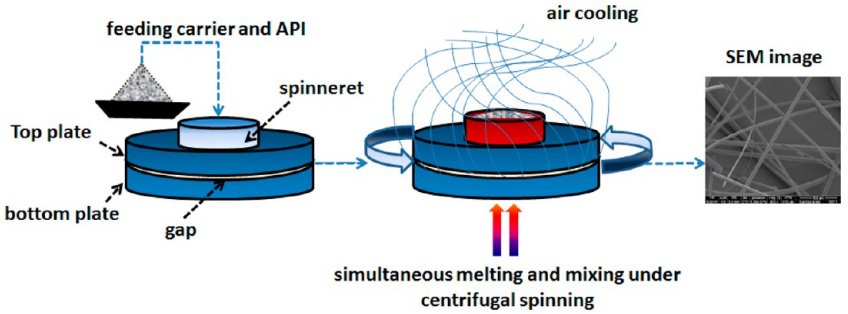

Figure 1. Schematic representation of the centrifugal spinning apparatus and individual process steps in the preparation of drug-loaded microfibers. Reproduced from ref 7. Copyright 2016 Elsevier.

of the microfibers formed. However, because of the particularly hygroscopic nature of amorphous sucrose, the shelf life of microfibers produced using this technique is expected to be relatively short. Physicochemical instability of amorphous solid dispersions is indeed one of the major challenges for this type of formulation, and this instability has been reported to have a detrimental effect on the drug dissolution rate and solubility during storage of these products.[8] Therefore, a significant effort has recently been directed toward stabilizing the drug in the amorphous state, particularly focusing on inhibiting recrystallization by the use of appropriate polymers.[9−11] However, the dissolution advantage of the amorphous over the crystalline state has not always been demonstrated to be as clear-cut as predicted. For example, Save and Venkitachalam found that there was no significant differences in the dissolution rates of fully amorphous nifedipine in polyethylene glycol 4000 (PEG 4000) solid dispersions compared to the corresponding physical mixtures.[12] Similarly, Verheyen et al. demonstrated that simply mixing crystalline diazepam and temazepam with PEG-6000 showed the same dissolution rates as the equivalent amorphous solid dispersion formulations.[13] In other studies, Pina et al. found that fully amorphous olanzapine in polyvinylpyrrolidone/vinyl acetate (PVP/VA) solid dispersions displayed comparable dissolution rates with the corresponding formulations containing crystalline olanzapine.[14] In a similar fashion, Andrews et al. found no difference in the dissolution performance between bicalutamide solid dispersions in PVP tested immediately after manufacture and those tested after 6 months storage at 65% RH/20 °C, despite the presence of drug crystals on the surface of aged samples.[15]

These discrepancies may potentially be linked to recrystallization of amorphous drugs upon contact with water, whereby rapid crystallization can occur as a result of an increase in the overall molecular mobility, rendering the dissolution behavior more comparable with material that was initially crystalline.[16] Moreover, examination of the literature of monolithic solid dispersions indicates examples of where moisture-induced recrystallized systems may actually show enhanced dissolution performance.[15,17−20] For example, recent work conducted by Chan et al. showed that after a deliberate early moisture-induced recrystallization of amorphous spray-dried ketoprofen and piroxicam in poly(vinyl alcohol) (PVA) solid dispersions, the dissolution performance was higher for the moisture-treated samples than the corresponding amorphous freshly prepared samples.[17] Moreover, the same authors showed that the apparent solubility of both drugs from the treated samples was about 5-fold higher than the equilibrium solubility of the equivalent pure drugs. Similarly, the dissolution rate of a ternary solid dispersion of diazepam in PEG 3000 and lactose was found to be faster after moisture-induced recrystallization at 75% RH/40 °C compared to the equivalent sample stored at 0% RH and at room temperature.[20] It is conceivable that these increases may be associated with the recrystallization process from or within the solid dispersion resulting in dissolution advantages in terms of, for example, surface area.[21] It is also feasible that the water sorption/desorption processes occurring during recrystallization under high relative humidity conditions may induce disordering of the drug crystal lattice, including formation of point defects, growth banding, vacancies, and dislocations.[22] Similarly, the presence of excipients have been found to strongly inhibit drug crystal growth rate, commonly by adsorbing onto the drug crystal surfaces, resulting in a diversification of drug crystal sizes, shapes, and solubility.[23] Overall, however, there does appear to now be a number of studies whereby the paradigm of amorphous systems holding an inevitable dissolution advantage over the crystalline equivalent does not appear to be wholly supported by observation.

The objective of this study is to investigate the effect of increasing relative humidity conditions (11, 33, 54, and 75% RH/25 °C) on the stability, recrystallization behavior, and dissolution performance of three microfibrous amorphous solid dispersion systems, consisting of the poorly water-soluble drugs olanzapine (OLZ), piroxicam (PRX), and itraconazole (ITZ) (all BCS class II drugs) in sucrose microfibers at a fixed drug loading (10% w/w). As the solid-state stability and final dissolution performance may potentially be affected by their physicochemical properties, the model drugs were chosen on the basis of their lipophilicity (log P) and molecular weight (M_w) in the increasing order of OLZ (M_w = 312.43 g/mol, log P = 2.2[24]) < PRX (M_w = 331.35 g/mol, log P = 3.06[25]) < ITZ (M_w = 705.64 g/mol, log P = 5.66[26]), to investigate links between those properties and drug recrystallization tendency. We specifically focus on the effect of rapid recrystallization, observed for freshly prepared microfiber formulations when exposed to the highest humidity conditions (75% RH/25 °C) on potential changes in microfiber size, morphology, drug distribution, drug physical state, and dissolution performance. Dissolution tests were conducted under nonsink conditions to evaluate both dissolution kinetics and potential increase in apparent drug solubility. Our intention is to further develop the use of microfibers as viable solid dispersion delivery systems but also to further explore the influence of physical state on the dissolution properties of poorly water-soluble drugs.

2. MATERIALS AND METHODS

2.1. Materials. Olanzapine (M_w = 312.43 g/mol) was purchased from Myjoy Ltd. (India); piroxicam (M_w = 331.34 g/

DOI: 10.1021/acs.molpharmaceut.6b01126
Mol. Pharmaceutics 2017, 14, 1666−1680

mol) was purchased from Afine Chemicals Ltd. (China); itraconazole (M_w = 705.64 g/mol) was purchased from Watson Noke Scientific Ltd. (China); sucrose (M_w = 342.29 g/mol) was obtained from Sigma−Aldrich Co. (USA). All buffer salts used for the dissolution medium, as well as dimethyl sulfoxide (99.9%) (DMSO), acetonitrile (99.8%) (ACN), and sodium *n*-dodecyl sulfate (99%) (SDS), were purchased from Sigma-Aldrich (Germany). All other chemical regents were of analytical grade.

2.2. Methods. *2.2.1. Preparation of Microfibers by Temperature-Controlled Centrifugal Spinning.* Unloaded and 10% (w/w) drug-loaded sucrose microfibers were prepared as illustrated in Figure 1 using a previously described temperature-controlled centrifugal spinning device.[7] Physical mixtures (PMs) were prepared by mixing sucrose (90% w/w) and drug (10% w/w) in a mortar for 5 min. Ten grams of starting material were accurately weighed and placed into the spinneret, which was preheated to the required temperature. Optimal procedure conditions were carefully determined on the basis of melting (T_m) and degradation (T_{deg}) temperature values of raw materials alone and in their PMs to avoid material degradation and to obtain homogeneous systems. Spinning operations were conducted with a rotational speed of 2400 rpm at room temperature (25 ± 5.0 °C). Freshly prepared microfibers were collected and characterized within 24 h of preparation.

2.2.2. Stability Study. The effect of relative humidity on the stability profile and recrystallization behavior of unloaded and drug-loaded sucrose microfiber formulations (10:90% w/w) was investigated by storing three different batches for each formulation in open glass vials at 25 ± 0.5 °C inside a desiccator containing saturated salt solutions to generate four different humidity conditions: lithium chloride (11% RH), magnesium chloride (33% RH), magnesium nitrate (53% RH), and sodium chloride (75% RH), for up to 8 months. MTDSC and XRPD were used in combination every day for the first month and after 3, 6, and 8 months of storage to monitor changes in the physical state of the formulations during storage. Drug dissolution studies, SEM/ESEM-EDS images, SS-NMR, and ATR-FTIR were also conducted on microfibers stored for 8 months at 75% RH/25 °C and compared to those freshly prepared. A Q5000 SA Dynamic Vapor Sorption Analyzer (DVS) (TA Instruments, New Castle, DE, USA) was also used to quantify and evaluate the water sorption tendency of freshly prepared samples at equilibrium under specific controlled humidity and temperature conditions. Five to seven milligrams of samples was placed on a metal coated quartz DVS pan at 25 °C and dried at 0% RH for 3 h. Samples were subsequently exposed to 33% RH for 24 h to evaluate the extent of moisture absorption.

2.2.3. Thermal Analysis. Thermal analysis of freshly prepared and aged samples was conducted using modulated temperature differential scanning calorimetry (MTDSC) (TA Instruments Q2000, New Castle, DE, USA) with a refrigerated cooling system attached to an inert dry nitrogen sample purge flow at 50 mL/min. Temperature calibration was performed using indium, *n*-octadecane, and tin; heat capacity constant calibration was performed using aluminum oxide TA sapphire disks at 2 °C/min with ±0.212 °C modulation amplitude over a 60 s period. All DSC and MTDSC experiments and calibrations were performed using a PerkinElmer 40 μL aluminum pan accompanying a pinholed lid. DSC experiments were performed on starting materials at 2 °C/min over an appropriate temperature range, while MTDSC experiments were conducted on all other samples at 2 °C/min with ±0.212 °C modulation amplitude over a 60 s period. The glass transition (T_g) values were measured in the reheating cycle and determined as the fictive glass transition temperature. Following the method developed by Barandiaran and Colmenero,[27] the drug glass forming ability/recrystallization tendency was evaluated by weighing a 1−3 mg sample into hermetically sealed pans, heating at 10 °C/min to 5 °C above the melting temperature, holding isothermally for 3 min, cooling at a rate of 20 °C/min to −70 °C and reheating at 10 °C/min to just above the melting temperature.[28] Water content and thermal decomposition temperature (T_{deg}) of both raw materials and formulations were measured using thermogravimetric analysis (TGA) with a Q5000 (TA Instruments, Newcastle, DE, USA). Samples were heated from room temperature up to 100 °C with a heating rate of 10 °C/min and held isothermally for at least 15 min before continuing the heating ramp up to 300 °C. The amount of water content was quantified as the percentage of mass loss observed in the temperature region below the onset of degradation. The data obtained were analyzed using the TA Instruments Universal Analysis 2000 software, version 4.7. All experiments were conducted in triplicate.

2.2.4. X-ray Powder Diffraction (XRPD). Ambient X-ray powder diffraction (XRPD) measurements were performed using a MiniFlex diffractometer (RigaKu, Tokyo, Japan). Samples were lightly pressed into 20 mm aluminum sample trays and the surface scraped evenly using a glass slide. A Cu Kα radiation point source (λ = 1.5148 227 Å) was operated at 40 mV and 15 mA. XRPD patterns were recorded using diffraction angles (2θ) from 5° to 50° (step size 0.05°; time per step 0.2 s). Data was exported and analyzed using OriginPro 2016. All experiments were conducted in triplicate.

2.2.5. Scanning Electron Microscopy (SEM). The morphology and size of freshly prepared microfibers and corresponding aged samples were analyzed using a Quanta 200F instrument (FEI, Hillsborough, OR, USA). Samples were coated with 20 nm of gold under vacuum using a Quorum Q150T Turbo-Pumped Sputter Coater (Quorum Technologies, UK). Data were collected over a selected area of the surface of samples. The average diameter and the percentage frequency of the microfibers were determined from the mean value of 100 individual measurements collected by analyzing the SEM micrographs using ImageJ (USA, version 1.46r). After storage at 75% RH/25 °C for 8 months, fibers collapsed into elongated particles with high aspect/ratio (length/diameter). Therefore, average particle size of the aged samples was estimated by measuring the length of the short axis diameter (shortest distance between two points) on a given particle using ImageJ.

2.2.6. Environmental Field Scanning Electron Microscopy (ESEM) and Energy-Dispersive X-ray Spectroscopy (EDS). Surfaces of the freshly prepared and aged microfibers (at 75% RH/25 °C) were scanned using a FEI/Philips XL-30 Environmental Field Emission scanning electron microscope (ESEM) (accelerating voltage 10 kV), equipped with a Schottky-based gun design using a point-source cathode of tungsten, which has a surface layer of zirconia (ZrO_2). Samples were fixed on sample stubs using double-sided adhesive tape. A sputter carbon coater (Quorum Technologies, Newhaven, UK) was used to coat the surfaces prior to imaging. EDS (INCA Energy manufactured by Oxford Instruments) connected to the ESEM was used to map the distribution of drug clusters using

DOI: 10.1021/acs.molpharmaceut.6b01126
Mol. Pharmaceutics 2017, 14, 1666−1680

Table 1. Experimental Operating Conditions Used for the Preparation of Microfibers and the Corresponding Glass Transition Values (T_g) Measured Using MTDSC and Drug Loading and Drug Loading Efficiency Determined Using eq 1

formulation	spinning condition		T_g (mean ± SD) (°C)	drug loading (% w/w)	drug loading efficiency (mean ± SD) (%)
	temperature (°C)	rotating speed (rpm)			
sucrose fibers	197	2400	71.1 ± 4.3		
OLZ−sucrose fibers	200	2400	73.9 ± 2.1	10	101 ± 2.3
PRX−sucrose fibers	205	2400	69.6 ± 1.4	10	97 ± 1.5
ITZ−sucrose fibers	197	2400	74.3 ± 1.9	10	99 ± 3.1

chlorine (Cl) in ITZ and sulfur (S) in OLZ and PRX as specific markers. Samples were tested using both ESEM and mapping mode EDS.

2.2.7. Drug Content and Loading Efficiency. Drug content was measured by dissolving predried samples, containing 10 mg of theoretical equivalent of drug content, in 5 mL of DMSO, in which both drug and carrier are soluble, followed by dilution in phosphate buffer (pH: 6.8) for UV detection at 254 and 353 nm for OLZ and PRX, respectively. For ITZ, predried samples were dissolved in 100 mL of 50:50 ACN/phosphate buffer (pH: 6.8) and analyzed using HPLC-UV system at 264 nm (Hewlett-Packard 1050 Series, Agilent Technologies, UK), equipped with a Synergi 4 μm Polar-RP 80 Å, 50 × 3 mm column (Phenomenex, UK). The system was operated under gradient flow at 1 mL/min using 50:50 ACN/water−acetic acid 0.1 (% v/v) as the mobile phase. For a detection wavelength of 264 nm, the ITZ peak elution time was 6.3 min. The standard curve linearity was verified from 1 to 100 μg/mL with an r^2 value of at least 0.999. Drug loading efficiency (DLE) was measured using eq 1:

$$\mathrm{DLE}(\%) = \frac{\text{amount of drug measured}}{\text{theoretical amount of drug based on drug loading}} \times 100 \quad (1)$$

2.2.8. Attenuated Total Reflectance-Fourier Transform Infrared Spectroscopy (ATR-FTIR). Characterization of PMs and formulation molecular structure was performed using attenuated total reflectance Fourier transform infrared spectroscopy (ATR−FTIR) (Bruker Vertex 90 spectrometer, UK). Measurements were performed with a resolution of 2 cm^{-1}, 32 scans over 4000−700 cm^{-1} range at room temperature (25 °C) in transmission mode. Spectra were analyzed using Opus software version 7.2 and OriginPro 2016. All experiments were conducted in triplicate.

2.2.9. Solid-State ^{13}C NMR Spectroscopy (SSNMR). Solid-state NMR experiments were carried out on Bruker Avance 300 spectrometer with a 7.05 T wide-bore magnet at ambient probe temperature. High-resolution solid-state ^{13}C was recorded at 75.5 MHz using a standard Bruker 4 mm double-resonance magic-angle spinning (MAS) probe. Solid materials were packed into zirconia rotors of 4 mm external diameter and spun at the MAS frequency of 8 kHz with stability better than ±3 Hz. High-resolution solid-state ^{13}C NMR spectra were recorded using cross-polarization (CP), MAS, high-power proton decoupling, and total suppression of sidebands (TOSS). Typical acquisition conditions for ^{13}C CPMAS TOSS experiments were ^{1}H 90° pulse duration = 2.45 μs; contact time = 2 ms; recycle delay = 5 s. Dipolar-dephased ^{13}C CPMAS TOSS spectra (also known as NQS CPMAS TOSS, where NQS stands for nonquaternary suppression) were also acquired in order to emphasize peaks due to nuclei, which are either remote from protons or have substantial motional averaging of dipolar interactions with protons. The dephasing delay used was 40 μs. ^{13}C chemical shifts are given relative to tetramethylsilane, which was calibrated using glycine (176.46 ppm).

2.2.10. Nonsink Dissolution Testing. Dissolution−supersaturation profiles of the formulations were obtained by nonsink dissolution tests in phosphate buffer (pH: 6.8) using a shaking incubator. For ITZ, 0.1% (w/v) of sodium dodecyl sulfate (SDS) was added to the dissolution medium. Samples containing 10 mg of drug were loaded into 50 mL of dissolution medium. One milliliter of samples was withdrawn at predetermined time intervals and filtered through a 0.22 μm Millipore Millex GT filter. The drawn volume was replaced with the same amount of blank dissolution medium from a separate vessel, also held at a temperature of 37 ± 0.2 °C. The absorbance of the filtrate was measured by UV (for OLZ, PRX) and HPLC-UV system (for ITZ) after appropriate dilution. Dissolution tests were performed for 25 h.

2.2.11. Statistical Analysis. The maximum drug concentration in solution (C_{max}) and the time of its occurrence (T_{max}) were obtained from the drug concentration−time profiles. Moreover, the supersaturation profiles between formulations were compared by measuring the area under the curve (AUC). All results are expressed as mean ± SD. The data from different formulations were compared for statistical significance by one way analysis of variance (ANOVA) and Tukey−Kramer posthoc test when $p < 0.05$.

3. RESULTS AND DISCUSSION

3.1. Sample Preparation. Temperature-controlled centrifugal spinning represents an innovative approach to solvent-free spinning of fiber-based fully amorphous solid dispersions with high production rates.[7] During the formation of fibers using this approach, materials are quickly mixed, melted, and stretched into fine fibers under simultaneous centrifugal and air friction forces. Both the enhanced surface area and amorphous nature of the product potentially improve dissolution performance of BCS class II drugs.[7] Fully amorphous (as determined using XRPD, data not shown) OLZ−, PRX−, and ITZ−sucrose microfibers with 10% (w/w) drug loading were successfully prepared using the operating conditions summarized in Table 1, these being chosen on the basis of melting (T_m) and degradation (T_{deg}) temperature values of each component and their corresponding physical mixtures. T_m values for the raw materials and in their PMs with sucrose were observed at 191 ± 0.5, 196 ± 0.4, 203 ± 0.2, and 169 ± 0.3 °C for sucrose, OLZ, PRX, and ITZ, respectively. T_{deg} values, determined using TGA, were observed at 230 ± 4.1, 234 ± 1.0, 232 ± 3.2, and 238 ± 3.7 °C for sucrose, OLZ−sucrose, PRX−sucrose, and ITZ−sucrose PMs, respectively. In addition, Table 1 summarizes experimental values of glass transition temperature (T_g) measured using MTDSC (in reheating cycle), drug loading, and drug loading efficiency of the fibers formed. It is noteworthy that the T_g values for the three systems are very

DOI: 10.1021/acs.molpharmaceut.6b01126
Mol. Pharmaceutics 2017, 14, 1666−1680

similar; this is expected from the similar reported T_g values of the drugs alone (71 ± 0.5, 61 ± 0.4, and 59 ± 0.2 °C for OLZ, PRX, and ITZ, respectively). Also note that SEM images and other basic characterization data are reported in a subsequent section.

3.2. Stability Studies. *3.2.1. Visual Observations.* Initially, freshly prepared microfibers were characterized and tested within 24 h of preparation and stored in sealed bags under ambient conditions; previous studies indicated a significant dissolution advantage for such systems,[7] and these are further explored for the systems below. However, preliminary observations suggested that the physical shelf life of these samples is relatively short; the instability was particularly apparent for drug-free sucrose microfibers which collapsed, liquefied, and then solidified into hard lumps of sucrose crystals within one or 2 days. This is in agreement with a previous study, whereby fully amorphous sucrose fibers were shown to collapse and crystallize in 1−3 days when exposed to 33% or higher RH conditions.[29]

The corresponding microfiber samples containing 10% (w/w) drug did not show any visible structural changes over 1−4 weeks under the same conditions. As the structural collapse began, it was observed that the drug-loaded samples broke down into dry and very fine powders instead of the hard and sticky clusters observed for the drug-free sucrose samples. Similar effects were observed for all three drugs. Based on these preliminary observations, we can assume that the presence of the drugs, even at relatively low drug loading, affects the crystallization tendency and structural collapse mechanism of the pure sucrose system.

3.2.2. Effect of Relative Humidity on the Time to Recrystallization of Microfibers. For a better understanding of the effect of moisture and the presence of the drugs on the physicochemical stability of drug-free and drug-loaded sucrose microfibers, samples were exposed to four different controlled relative humidity conditions (11, 33, 53, and 75% RH) at 25 °C and periodically characterized over an 8 month period.

The physical state of all samples after exposure to moisture was monitored using XRPD and MTDSC. Samples were considered fully amorphous if showing only one single, mixed-phase glass transition (T_g) from the MTDSC profiles and a broad halo pattern from the XRPD diffraction patterns. As an example, Figure 2A,B shows MTDSC and XRPD results for all samples exposed for 8 months to 25 °C/11% RH. It can be seen that all samples exposed to 11% RH maintained their amorphous state over an 8 month period, demonstrated by a mixed-phase glass transition (T_g) from the MTDSC traces and a broad halo pattern from the XRPD diffractograms. T_g values were found to be equivalent to samples characterized immediately after preparation, suggesting good long-term stability in the amorphous state under these conditions. However, at higher relative humidity conditions, the stability of all samples in the amorphous state is compromised. The appearance of Bragg peaks from the XRPD diffractograms was considered as clear evidence of recrystallization. MTDSC was mainly used to confirm that recrystallization occurred based on the disappearance of the T_g of the relative component.

Table 2 summarizes the sample physical stability data under the aforementioned humidity conditions, and the time range in which each sample shows evidence of recrystallization based on the appearance of Bragg peaks (from the XRPD data) as well as the disappearance of the T_gs together with the corresponding exothermic crystallization events. When both requirements

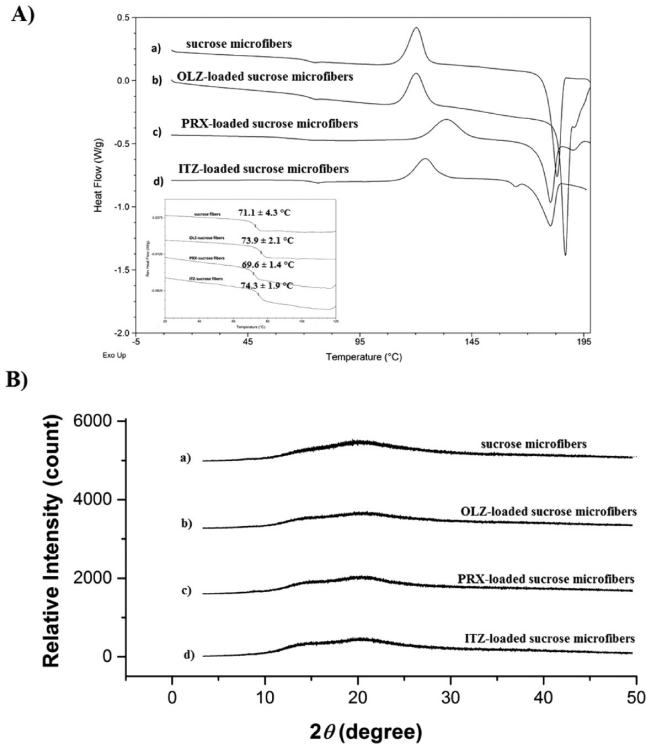

Figure 2. (A) MTDSC heat flow traces and (B) XRPD diffractograms of amorphous microfibers after 8 months storage at 11% RH/25 °C of (a) drug-free sucrose microfibers, (b) OLZ-loaded sucrose microfibers, (c) PRX-loaded sucrose microfibers, and (d) ITZ-loaded sucrose microfibers with inset view showing magnification of glass transitions analyzed with reversing heat flow. All microfibers contained 10% (w/w) drug loading.

were satisfied, an average number of days ± SD was reported. Inspection of this table indicates that the two techniques are in reasonable agreement, providing a relatively narrow time range in which the recrystallization process begins, although not without discrepancies. In particular, the XRPD data of all recrystallized samples suggest that only sucrose recrystallized out from the amorphous systems as only Bragg peaks corresponding to crystalline sucrose were detected, likely due to poor sensitivity of the instrument in detecting low amount of drugs. However, MTDSC profiles of the same samples collected at the same time range showed no amorphous content by the absence of any detectable T_g, suggesting that also the drugs together with sucrose might have recrystallized. Moreover, prior to the complete disappearance of T_gs from the MTDSC profiles, T_gs for all systems were seen to become broader and gradually decrease due to the plasticizing effect of sorbed water. However, for better clarity, in this section the term recrystallization refers to sucrose recrystallization only as from the data collected using the two techniques, we can only provide evidence for the physical state of sucrose. These discrepancies between XRPD and MTDSC are further discussed in section 3.4.3. Upon exposure to 54% RH/25 °C and 75% RH/25 °C, all samples collapsed and sucrose recrystallization occurred within 24 h. Again, a more in-depth analysis of the actual physical state for the three drugs under the highest humidity conditions (75% RH/25 °C) is provided in a subsequent section.

However, it is interesting to note that samples exposed to 33% RH/25 °C showed significant differences in sucrose

DOI: 10.1021/acs.molpharmaceut.6b01126
Mol. Pharmaceutics 2017, 14, 1666−1680

Table 2. Average Time Required for the Onset of Sucrose Recrystallization for All Formulations Stored under 11, 33, 53, and 75% RH at 25 °C, Measured by MTDSC and XRPD, $n = 6$[a]

sample	relative humidity (%)	XRPD profiles	T_g (mean ± SD) (°C)	onset of sucrose recrystallization time (mean ± SD) (days)
sucrose fibers	11	halo pattern	71.1 ± 4.3	n.o.
	33	sucrose Bragg peaks	n.o.	**2.1 ± 0.8**
	53	sucrose Bragg peaks	n.o.	0.8 ± 0.2 (<1 day)
	75	sucrose Bragg peaks	n.o.	0.7 ± 0.1 (<1 day)
OLZ−sucrose fibers	11	halo pattern	73.9 ± 2.1	n.o.
	33	sucrose Bragg peaks	n.o.	**23.5 ± 2.6**
	53	sucrose Bragg peaks	n.o.	1.1 ± 0.2
	75	sucrose Bragg peaks	n.o.	0.9 ± 0.1
PRX−sucrose fibers	11	halo pattern	69.6 ± 1.4	n.o.
	33	sucrose Bragg peaks	n.o.	**9.0 ± 1.6**
	53	sucrose Bragg peaks	n.o.	1.0 ± 0.2
	75	sucrose Bragg peaks	n.o.	0.8 ± 0.1
ITZ−sucrose fibers	11	halo pattern	74.3 ± 1.9	n.o.
	33	halo pattern	74.1 ± 2.1	**n.o.**
	53	sucrose Bragg peaks	n.o.	1.7 ± 0.8
	75	sucrose Bragg peaks	n.o.	1.1 ± 0.1

[a]Bold values highlight significant differences ($p < 0.05$) in the sucrose recrystallization times under 33% RH. n.o. = not observed. Crystalline sucrose 2θ angle peaks: 11.64°, 13.10°, 18.78°, 19.56°, and 24.70°.

recrystallization time. As shown in Table 2 (bold values), the onset time range for sucrose recrystallization varied among samples. In particular, we can identify three distinct cases under these conditions: relatively rapid sucrose recrystallization for drug-free sucrose microfibers (2.1 ± 0.8 days), ∼8-fold and ∼2-fold slower recrystallization in the presence of OLZ (23.5 ± 2.6 days) and PRX (9.0 ± 1.6 days), respectively, and inhibition of recrystallization in the presence of ITZ for the duration of the stability study (8 months).

Overall, the addition of the model drugs resulted in a significant delay in sucrose recrystallization time from the microfibers, suggesting dramatic reductions in the system molecular mobility in the solid state; this may be through molecular interactions, alterations in T_g via plasticization effects, or alterations in the water uptake tendency. In a study conducted by Shamblin and Zografi, the recrystallization of sucrose from the amorphous state was found to be inhibited by the presence of 50 (%w/w) PVP, prepared as amorphous lyophilized solid solutions.[30] The inhibiting effect could not be attributed to the antiplasticizing effect of PVP as T_g values of the mixtures remained unchanged, but due to coupling of sucrose to PVP through hydrogen bonding, which reduced the local molecular mobility of sucrose. Sucrose molecules with eight hydroxyl groups, three hydrophilic oxygen atoms, and 14 hydrogen atoms can interact through hydrogen bonding with proton acceptor/donor sites present in OLZ, PRX, and ITZ. As shown in our previous work, ATR-FTIR spectra of OLZ-loaded microfibers displayed a chemical shift of ν(C−N) (piperazinyl ring of OLZ) to lower wavenumber indicating potential hydrogen bonding interactions between OLZ and sucrose molecules.[7] However, no chemical shifts were observed in the case of PRX- and ITZ-loaded sucrose microfibers as discussed in more detail in section 3.4.4. This may reflect why the addition of PRX did not stabilize the system as well as OLZ. However, these observations are not sufficient to explain the significant inhibition effect in the sucrose recrystallization observed at 33% RH after the addition of ITZ.

3.3. Assessment of Water Uptake in Relation to Drug Crystallization Tendency. Another possible cause of the significantly slower sucrose recrystallization tendency observed for ITZ-loaded microfibers stored at 33% RH may be related to the different degrees of lipophilicity of the model drugs. The addition of the more lipophilic ITZ (log P = 5.66)[26] compared to OLZ (log P = 2.2)[24] and PRX (log P = 3.06)[25] may account for the greater recrystallization inhibition observed for the ITZ−sucrose system. Molecularly dispersed lipophilic ITZ molecules may increase the overall hydrophobicity of the sucrose microfiber surfaces, slowing the diffusion of the water into the hydrophilic sucrose domains and therefore inhibiting crystallization.

If this assumption is true, ITZ−sucrose systems should absorb less water during storage than the other samples. Therefore, the water uptake profiles of samples were measured using DVS after allowing equilibration at 25 °C and 33% RH for 24 h after preparation. As expected, no crystallization was observed over the time scale of the experiment. Drug-free sucrose microfibers were indeed found to significantly ($p < 0.05$) absorb higher amounts of water (5.3 ± 0.5%) compared to the drug-loaded sucrose systems in the decreasing order of OLZ−sucrose (3.4 ± 0.3%) > PRX−sucrose (2.9 ± 0.4%) > ITZ−sucrose (1.79 ± 0.2%). Overall, these findings suggest that drug-loaded microfibers are more resistant to the absorption of water under these conditions than the pure sucrose microfibers and that the higher lipophilicity of ITZ results in a lower uptake than the less lipophilic OLZ or PRX.

In addition, it is perfectly feasible that the superior ability of ITZ-loaded microfibers to remain in the amorphous state upon storage compared to OLZ− and PRX−sucrose systems may be linked to the drug glass-forming abilities and the corresponding devitrification tendencies. As a first simple observation, the more complex and larger molecular structure of ITZ (M_w = 705.64 g/mol) compared to those of OLZ (M_w = 312.43 g/mol) and PRX (M_w = 331.35 g/mol) is generally indicative of stronger glass formation and hence greater likelihood of remaining in the amorphous state.[28,31]

For a more precise indication of drug crystallization tendency we used the DSC screening method, whereby drugs can be separated into three distinct classes based on their thermal response upon cooling from the undercooled melt or upon reheating from the glassy state.[28] OLZ and PRX were found to

DOI: 10.1021/acs.molpharmaceut.6b01126
Mol. Pharmaceutics 2017, 14, 1666−1680

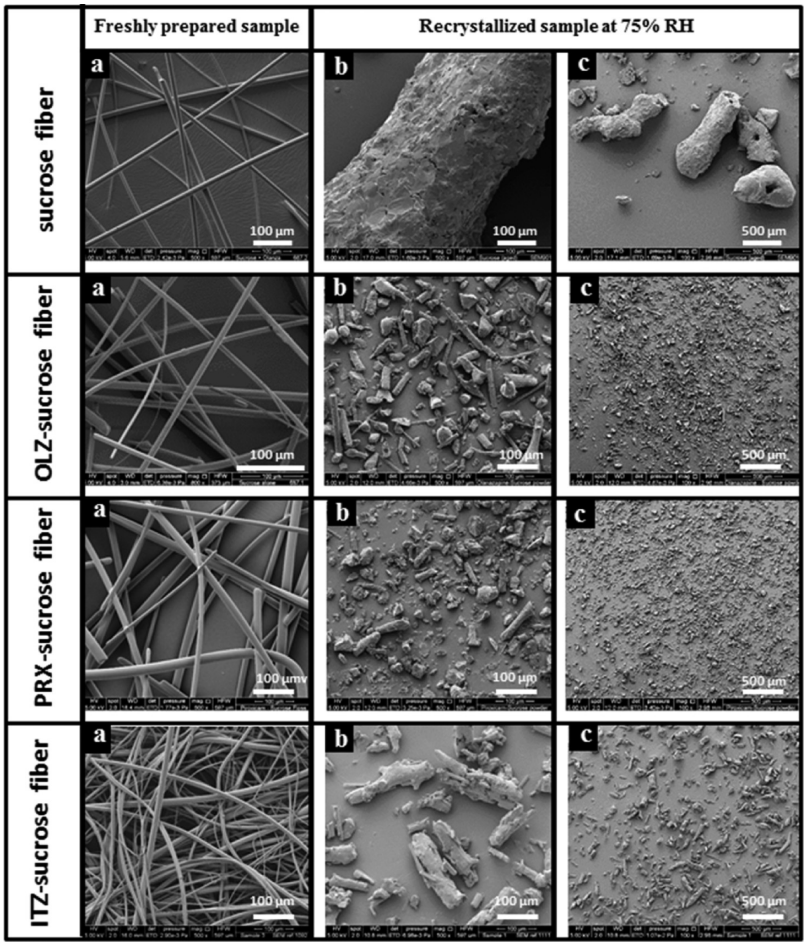

Figure 3. SEM images of the surface morphology of all samples: (a) freshly prepared samples (500× magnification), (b) 8-month aged samples (500× magnification), and (c) 8-month aged samples (100× magnification). All aged samples were stored at 75% RH/25 °C for 8 months.

fall into class II as recrystallization was not observed upon cooling from the undercooled melt, but it was observed during reheating above the corresponding T_g. For ITZ, no crystallization was observed either upon cooling or reheating up to the melting point (class III), clearly indicating a stronger resistance to devitrification compared to OLZ and PRX (data not shown).

Overall, therefore, there are a number of possible explanations for the greater stability of the drug loaded systems compared to the unloaded and the rank order of the three incorporated drugs; these include direct molecular interaction, lipophilicity with associated lower water uptake, and intrinsic crystallization tendency of the incorporated drug. The anomalous behavior of the ITZ systems is of particular interest and is most probably linked to the lower water uptake or the intrinsic crystallization properties of the drug (or a combination of both).

3.4. Solid-State Characterization of Microfibers Stored at 25 °C/75% RH. Since the main purpose of this study is to investigate the potential effects of a moisture-induced sucrose recrystallization on microfiber size, morphology, drug distribution, drug physical state, and dissolution performance, samples stored at 75% RH/25 °C were chosen for further analysis and investigations in order to allow comparison of the initial amorphous fibers with the equivalent moisture-treated systems.

3.4.1. Scanning Electron Microscopy (SEM). Figure 3 shows the scanning electron micrographs (SEM) of freshly prepared microfibers and the corresponding moisture-treated samples after 8 months of storage at 75% RH/25 °C. It is clear that storage results in both changes to the surface integrity and the fiber architecture, with the generation of elongated particles as the fiber structure collapses. SEM images collected after 1 day of storage did not show any significant difference in terms of morphology and size compared to those after 8 months of storage (data not shown). With the exception of some rounded particles, the majority of aged drug-loaded particles have visibly maintained the fiber shape, although shorter in length compared to the corresponding freshly prepared samples. As mentioned previously, it is clear from Figure 3 that the aged drug-free sucrose microfibers collapsed into significantly larger and more irregular crystal agglomerates compared to the aged drug-loaded samples. Table 3 shows the average fiber diameter of microfibers upon preparation and average particle size of the corresponding aged samples after storage. Crystal clustering and agglomeration observed for drug-free sucrose microfibers may be a result of the recrystallization mechanism of sucrose from the amorphous state. It has been reported that when amorphous sucrose recrystallizes, a relatively small amount of moisture is generally trapped in the crystal lattice due to the particularly high tendency of sucrose molecules to form hydrogen bonds with water.[32] This internal water is slowly released to the crystal surface, forming a residual thin layer of

DOI: 10.1021/acs.molpharmaceut.6b01126
Mol. Pharmaceutics 2017, 14, 1666−1680

Table 3. Fiber Diameter of Freshly Prepared Samples and Particle Size (Short Diameter Length) of the Corresponding Aged Samples after 8 Month Storage at 75% RH/25 °C

	freshly prepared sample	aged sample
sample	fiber diameter (mean ± SD) (μm)	particle size (mean ± SD) (μm)
sucrose fibers	9.77 ± 3.10	334.52 ± 86.58
OLZ–sucrose fibers	10.87 ± 2.94	17.10 ± 9.45
PRX–sucrose fibers	14.10 ± 4.53	15.43 ± 7.58
ITZ–sucrose fibers	5.84 ± 2.97	29.03 ± 7.20

supersaturated "syrup" on the surface of each crystal. This forms an external low-permeability crust of amorphous sugar, which is the main cause of caking and formation of large crystal aggregates.[33] However, the absence of significant crystal agglomeration for the aged drug-loaded sucrose microfibers supports previous observations that the drugs may interfere with the mechanism of recrystallization of amorphous sucrose. This might also explain why freshly recrystallized drug-loaded sucrose microfibers were found to retain negligible amount of water (~0.01%) compared to the pure recrystallized sucrose system (~2–3%), measured using TGA.

3.4.2. Assessment of Drug Distribution. It has been reported that the crystallization of sucrose can be inhibited by substances able to adsorb onto the sucrose crystal surface during crystallization.[34,35] These substances impede the bulk diffusion of sucrose molecules to the crystal surface and surface incorporation, preventing further growth or recrystallization. Therefore, energy-dispersive spectroscopy (EDS) was also conducted to evaluate the drug distribution within the sucrose matrix in drug-loaded microfibers before and after storage. This technique can distinguish and locate a specific chemical element present in a drug molecule, giving a distinct signal in the EDS spectrum.[36] Since chlorine (Cl) atoms are unique to ITZ and sulfur (S) atoms are unique to OLZ and PRX, these chemical elements were used as specific markers to track the drug distribution on the scanned surfaces.

Figure 4 shows the drug distribution (red dots) in the sucrose matrix as detected by EDS for all samples before (freshly prepared samples) and after 8 month storage at 75% RH/25 °C, respectively. Overall, the technique indicates that in all three cases the drug appears to be reasonably evenly distributed in the sucrose matrix, before and after storage and indeed present on the surface, bearing in mind that the technique has a penetration depth of approximately 0.16–1 μm at 10 kV.[37]

Nevertheless, looking at the freshly prepared samples there does appear to be some inconsistency in the color intensity for the OLZ system, when comparing different fibers in the scanned area, while for PRX there appears to be spots of intense color, which may indicate some degree of surface phase separation. However, it is important to note that a certain degree of phase separation may have occurred during the ESEM-EDS experiments given the environmental conditions associated with the measurements and the relative instability of the freshly prepared samples. However, ITZ system shows a more even drug distribution compared to PRX and OLZ systems, indicated by the absence of regions with different color intensity.

After collapse of the structures on storage, it is interesting to note that spots of intense color/drug become more visible for all three systems, particularly apparent for the particles containing OLZ and PRX. Of the three drugs, PRX again shows the greatest evidence for separation of the two components on crystallization, as seen by the presence of regions that show no coloration. Interestingly, ITZ shows a much more even distribution of drug than the other two samples, even after crystallization. Overall, therefore, the study indicates that the collapse process leads to particles, whereby

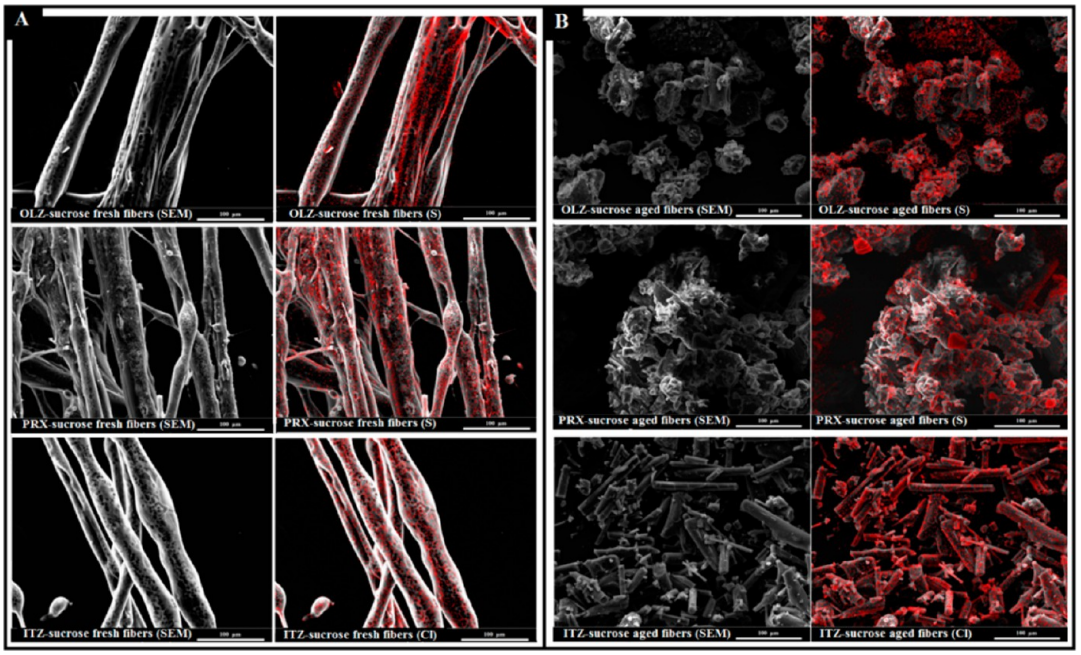

Figure 4. SEM micrographs of the areas mapped by EDS for all samples: (A) freshly prepared microfibers and (B) 8-month aged microfibers stored at 75% RH/25 °C. Red dots represent the distribution of the drugs by tracking sulfur (S) for OLZ and PRX, and chloride (Cl) for ITZ.

DOI: 10.1021/acs.molpharmaceut.6b01126
Mol. Pharmaceutics 2017, 14, 1666–1680

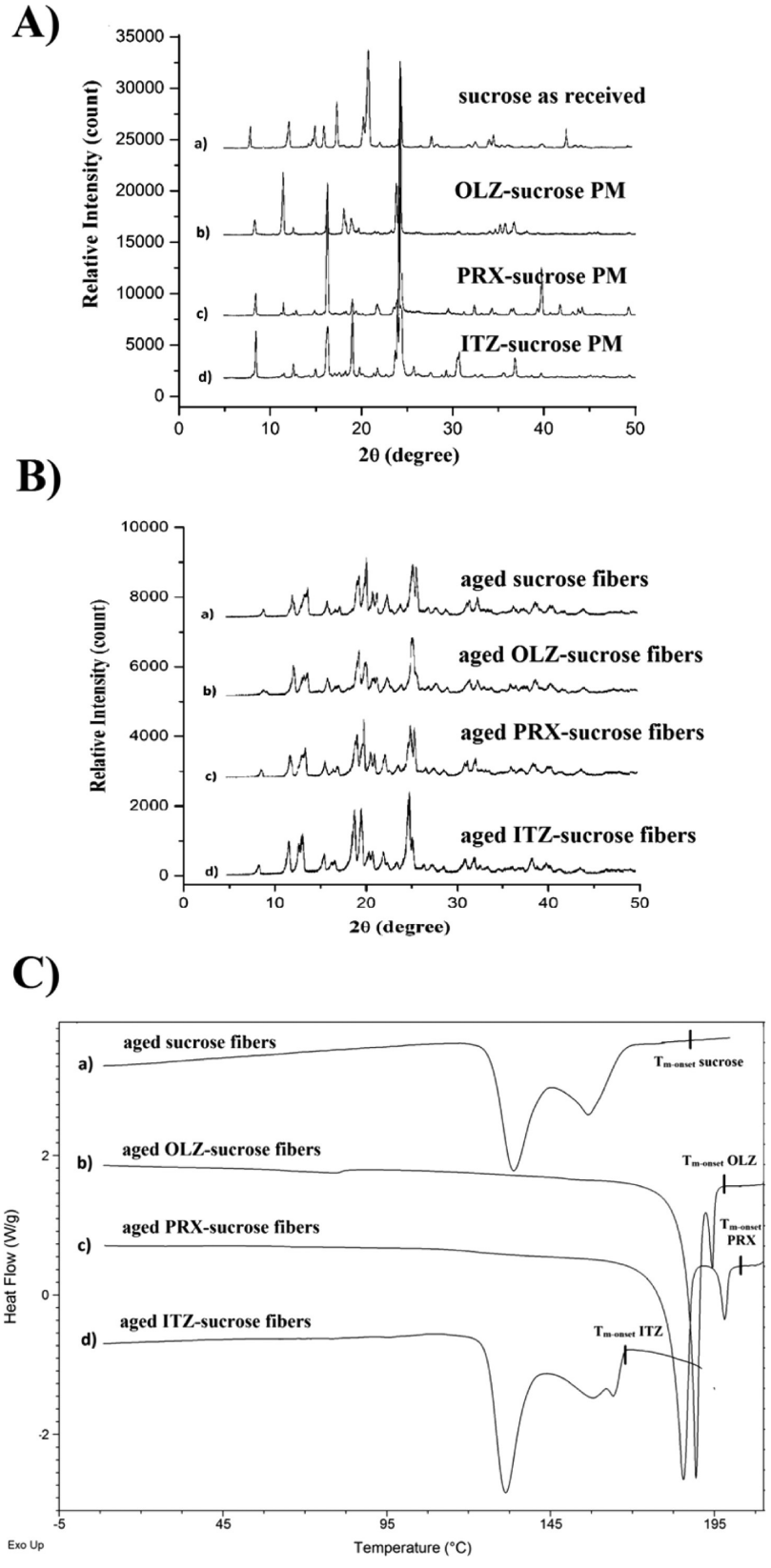

Figure 5. Powder X-ray diffractograms of (A) starting materials and (B) 8-month aged samples; (C) MTDSC traces of 8-month aged samples. All aged samples were stored at 75% RH/25 °C for 8 months.

the two components (drugs and sucrose) are present and mixed together. However, there appear to be some degree of separation into distinct crystalline regions, which may have some effects on the final drug dissolution performance.

3.4.3. Sample Crystallinity and Thermal Response. The crystallinity of aged fiber formulations was initially examined using XRPD and MTDSC. The diffraction patterns of aged drug-loaded fibers after 8 month of storage at 75% RH/25 °C,

DOI: 10.1021/acs.molpharmaceut.6b01126
Mol. Pharmaceutics 2017, 14, 1666−1680

are compared to the corresponding PMs and displayed in Figure 5A,B. The presence of diffraction peaks indicates that all formulations contain crystalline material. However, diffraction peaks are significantly broader with decreased intensities if compared to the corresponding PMs. Variations in the intensity of diffraction peaks are generally associated with the preferred crystallographic orientation of most materials. More importantly, as previously mentioned, characteristic peaks of all three drugs could not be detected from the diffraction patterns of the aged samples, showing only characteristic peaks of crystalline sucrose (11.64°, 13.10°, 18.78°, 19.56°, and 24.70°). In other words, XRPD data themselves confirm that, while sucrose completely recrystallized after storage, there appears to be less evidence of drug recrystallization. However, these findings may not be conclusive as this technique has several disadvantages associated with the preferred crystallographic orientations and peak broadening, as well as poor sensitivity in detecting components present in relatively lower ratios in a two phase system.

Figure 5C shows the MTDSC profiles of the aged samples after 8 month of storage at 75% RH/25 °C. In contrast to XRPD data, MTDSC profiles of the aged samples show that both components (drug and carrier) are present in the formulations. The absence of the glass transitions and exothermic crystallization, and the presence of endothermic melting peaks might indicate that both components of all samples recrystallized during storage. In the case of OLZ, however, a weak endotherm can be seen at around 80 °C, which cannot be associated with the glass transition of OLZ and may instead indicate water loss (see section 3.4.5). It is interesting to note that the onset of melting temperature values of each component from the aged samples are found to be depressed relative to the onset of melting peaks ($T_{m\text{-}onset}$) for the pure untreated materials (indicated by the annotations on each MTDSC trace and corresponding to 191 ± 0.5, 196 ± 0.4, 203 ± 0.2, and 169 ± 0.3 °C for sucrose, OLZ, PRX, and ITZ, respectively). This is particularly apparent for the aged sucrose in both drug-free and the ITZ−sucrose systems, which shows two broad peaks at significant lower temperatures ($T_{1m\text{-}onset}$, 126 ± 0.8 °C; $T_{2m\text{-}onset}$, 149 ± 0.4 °C) relative to that of intact sucrose. A similar behavior pattern has been reported by another author, whereby recrystallized sucrose showed a significant depression of its melting point, which was attributed to defects in the lattice structure.[38] If local defects, impurities, and/or submicron crystallites are present in the crystal lattice, the physicochemical properties, including the melting behavior, may be altered relative to the corresponding intact crystal.[39] These observations may indicate an overall reduction in the solid state intermolecular interactions, which in turn may affect the drug solubility and dissolution performance. Interestingly, there appears to be little or no change in the melting behavior of sucrose for the aged OLZ− and PRX−sucrose systems, showing only one sharp melting peak around 185−190 °C as would normally be expected for intact sucrose.

XPRD diffractograms and MTDSC profiles collected over the 8 month period under 75% RH/25 °C were totally reproducible and superimposable to those obtained after 1 day of storage at the same conditions, suggesting that no further changes of physicochemical properties of the recrystallized samples occurred during storage (data not shown).

3.4.4. Attenuated Total Reflectance-Fourier Transform Infrared Spectroscopy (ATR-FTIR). Although the MTDSC traces indicated that both drug and carrier recrystallized during storage, XRPD was not able to detect characteristic Bragg peaks of the drugs. Therefore, ATR-FTIR and SS-NMR (discussed in the next section) were used to further elucidate the physical state of the drugs and to observe whether potential changes in the drugs' molecular structure occurred as a result of storage. Figure 6A−C compares ATR-FTIR spectra of the freshly prepared drug-loaded microfiber formulations for OLZ, PRX, and ITZ in comparison with corresponding aged formulations, pure drugs, and PMs, respectively. To identify the presence of drugs, we particularly focused on the region between 1700 and

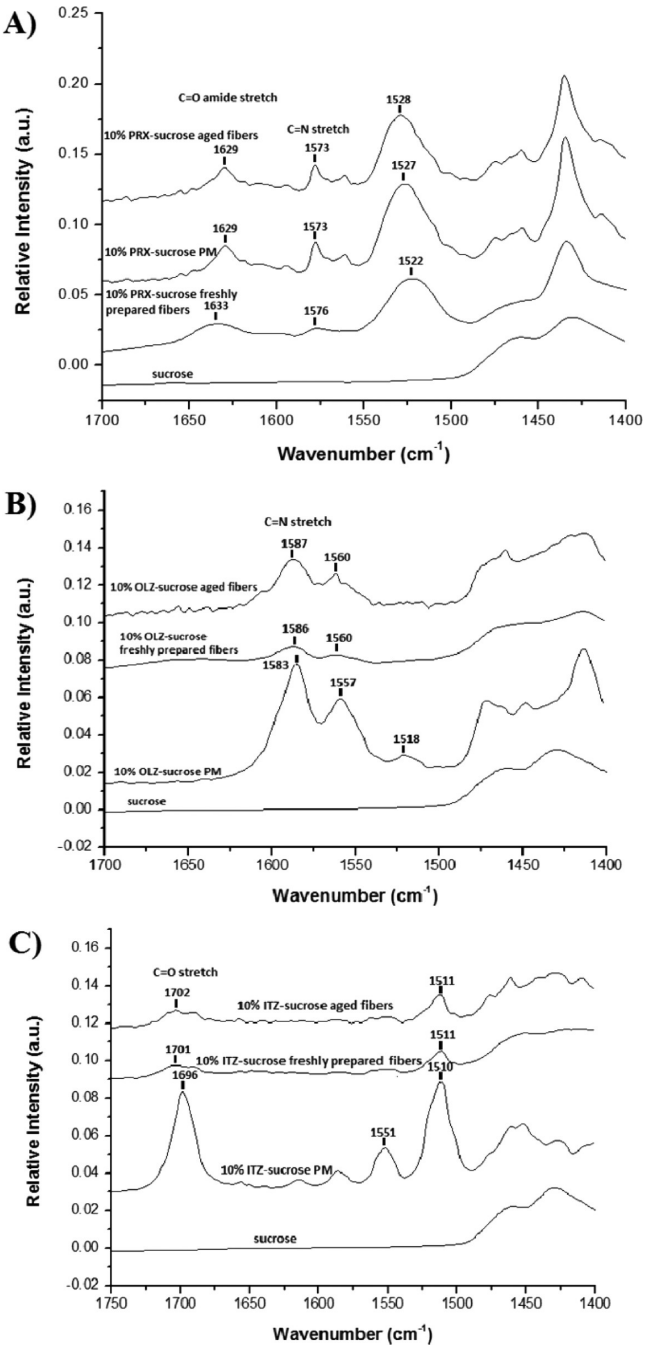

Figure 6. Comparison of ATR−FTIR spectra in the region between 1700 and 1400 cm^{-1} of drug-loaded freshly prepared samples, corresponding aged samples, PMs, and sucrose as received for (A) PRX, (B) OLZ, and (C) ITZ. All aged samples were stored at 75% RH/25 °C for 8 months.

DOI: 10.1021/acs.molpharmaceut.6b01126
Mol. Pharmaceutics 2017, 14, 1666−1680

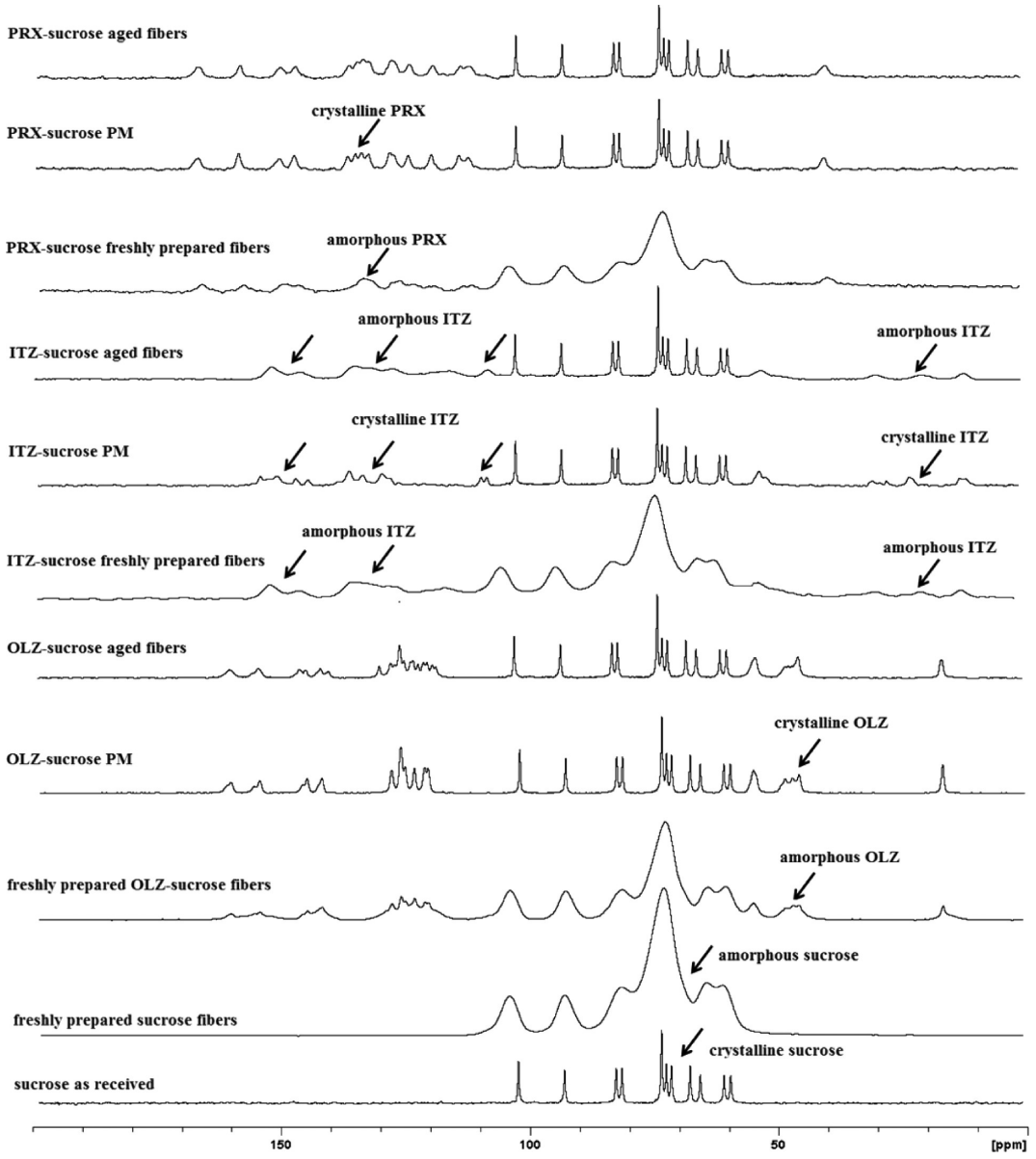

Figure 7. ^{13}C CP/MAS NMR spectra of freshly prepared microfibers, the corresponding aged samples, PMs, and sucrose as received. All aged samples were stored at 75% RH/25 °C for 8 months.

1400 cm^{-1} as sucrose shows no absorption in this region. In all cases, there are clear differences between the ATR-FTIR spectra of freshly prepared samples and the corresponding physical mixtures. Due to the amorphous character of freshly prepared fibers, characteristic peaks of all drugs were found to be fewer in number and broader relative to those of the corresponding drugs in their PMs. Regarding the aged samples, sharpening of characteristic peaks for all drugs is expected as a result of rapid recrystallization upon storage at 75% RH/25 °C as previously observed from DSC and XRPD results. Surprisingly, while it is clear from a comparison between aged samples and PMs that PRX crystallized into its previous crystalline form (Form I) (totally overlapping spectra), two distinct cases were observed for OLZ and ITZ. In the case of ITZ, there is no evidence of narrowing of peaks or any sign of recrystallization as the spectra of aged samples and corresponding freshly prepared samples are superimposable. This may suggest that ITZ did not recrystallize during storage. In the case of OLZ, although there seem to be a narrowing of peaks in the aged samples indicating recrystallization, peaks at 1582 and 1556 cm^{-1} assigned to ν(C═N) (azepine ring) and ν(C═C) (benzene and thiophene rings), respectively, appear at relatively higher frequencies in the aged sample compared to the corresponding PM. It is also interesting to note that the position of these peaks in the aged samples is equivalent of that observed in the amorphous freshly prepared samples. This may indicate that OLZ is either partially present in the amorphous state or, more likely, OLZ is present in a different crystalline form. In fact, OLZ has been found to exist in more than 25 possible crystalline forms.[40] In particular, in the presence of water and at ambient temperature, OLZ was found to easily convert (within hours) to the less soluble dihydrate B or the least soluble dehydrate D.[41] However, due to the very high concentration of sucrose and in turn the relatively low drug loading, the identification of a different form of OLZ was not possible using ATR-FTIR.

DOI: 10.1021/acs.molpharmaceut.6b01126
Mol. Pharmaceutics 2017, 14, 1666−1680

3.4.5. Solid-State ^{13}C NMR Spectroscopy (SSNMR). SSNMR spectroscopy is a powerful, nondestructive, and noninvasive technique, particularly effective for investigating the drug's physical state as well as polymorphism. Figure 7 shows ^{13}C CP/MAS NMR spectra collected for all freshly prepared samples, the corresponding aged samples, PMs, and sucrose as received. All PMs and unprocessed sucrose show sharp and highly resolved resonances associated with the well-defined solid-state environments of the ^{13}C nuclei in the crystal structures. Freshly prepared microfibers are completely amorphous as confirmed by the observed broad resonance lines (Figure 7). As an illustration, the half-height line width of the signal at ~103 ppm increases from 10 Hz in crystalline samples to 250 Hz in amorphous samples. In particular, differences between crystalline and amorphous PRX can be clearly seen at around 132−136 ppm (crystalline PRX, four peaks at 132.4, 133.7, 135.1, 136.5 ppm; amorphous PRX, one peak at 134.3 ppm). Similarly, significant differences between crystalline and amorphous ITZ can be seen at around 108−109 ppm (crystalline ITZ, two peaks at 108.0 and 109.5 ppm; amorphous ITZ, one peak at 108.2), 153−146 ppm (crystalline ITZ, three peaks at 153.7, 150.5, and 146.3 ppm; amorphous ITZ, one peak at 146.1), and 22 ppm (crystalline ITZ, one peak at 22.2 ppm; amorphous ITZ, one peak at 19.7 ppm). For OLZ, ^{13}C chemical shift of amorphous OLZ remained mostly unchanged relative to that of crystalline OLZ, although peaks in amorphous OLZ are broader, particularly evident at around 48−46 ppm (crystalline OLZ, three well-defined peaks at 48.5, 47.1, 46.0 ppm; amorphous OLZ, the same peaks are less resolved due to signal broadening). The SSNMR spectrum of PRX from the aged sample is readily assigned to that of crystalline PRX from the PM. This confirms that PRX recrystallizes into its previous form (Form I) during storage. However, in the case of OLZ−sucrose aged sample, although resolved resonances indicate that OLZ recrystallized during storage, the ^{13}C chemical shift is somewhat different to the SSNMR spectrum of crystalline OLZ (Form I) from the corresponding PM. In particular, additional resonances at 119.2, 119.8, 122.5, 130.4, 140.9, and 146.6 ppm were found in the crystalline OLZ from the aged samples, indicating the presence of one or more different crystal forms. The most relevant anhydrates and hydrates of OLZ have been previously characterized by ^{13}C CP/MAS NMR spectroscopy.[41] The analysis of the specific ^{13}C chemical shift and peak assignments for the relevant OLZ crystal forms indicates that some of the additional peaks found in the OLZ aged samples are identified to belong to dehydrate B. Therefore, OLZ may be present in a mixture of Form I and dehydrate B. This might also explain the first weak endotherm observed at around 82 °C in the MTDSC profile of aged OLZ−sucrose fibers in Figure 5C, which may be associated with the dehydration process of OLZ dehydrate as previously reported in the literature.[42] For ITZ, it is clear that the ^{13}C NMR chemical shifts and line widths of the drug in the aged sample are similar to those in the corresponding freshly prepared sample. This observation agrees well with the ATR-FTIR results, whereby ITZ did not recrystallize during storage.

3.4.6. In Vitro Dissolution Study. Figure 8A−C shows dissolution−supersaturation profiles (for OLZ, PRX, and ITZ, respectively), obtained under nonsink conditions for the freshly prepared microfiber formulations in comparison with corresponding aged samples at 75% RH/25 °C (both freshly recrystallized and after 8 month of storage), PMs, and pure drugs.

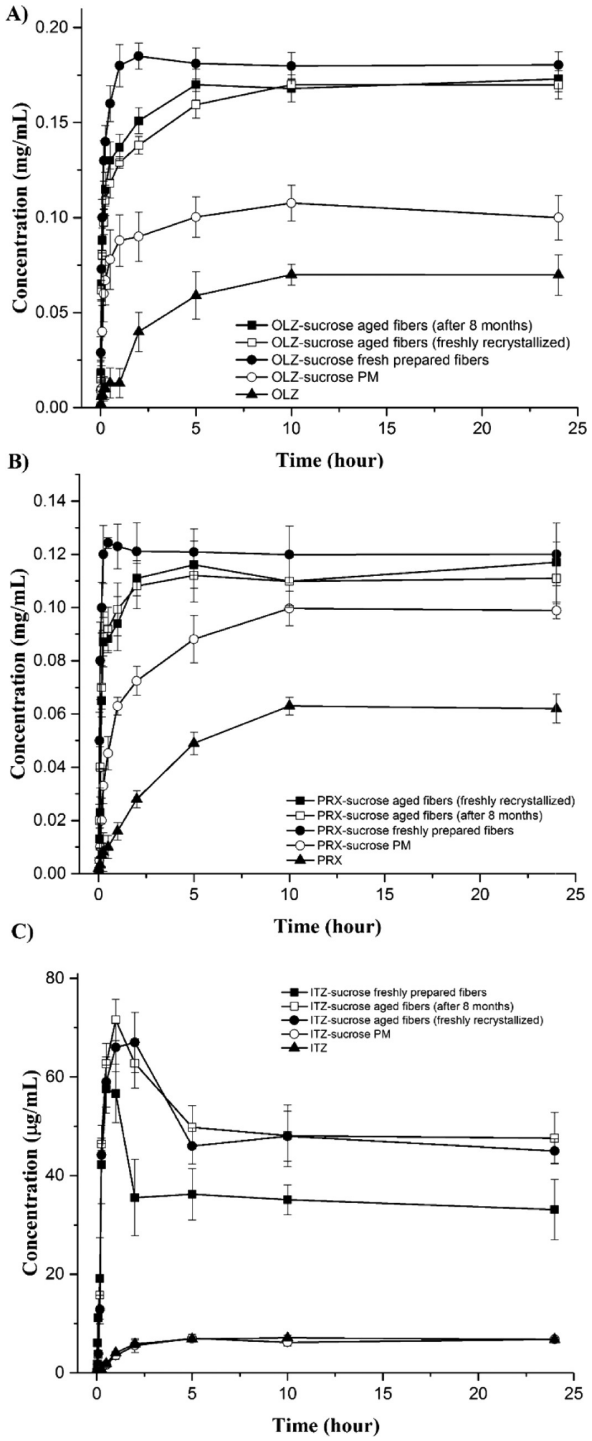

Figure 8. Comparison of dissolution−supersaturation profiles obtained under nonsink conditions between freshly recrystallized samples under 75% RH/25 °C, 8-month aged samples under 75% RH/25 °C, freshly prepared samples, PMs, and pure drug for (A) OLZ, (B) PRX, and (C) ITZ.

As shown in our previous work, freshly prepared OLZ- and PRX-loaded sucrose microfibers showed evidence for supersaturation, with sustained plateau levels under nonsink conditions; this is putatively ascribed to their amorphous nature, the enhanced surface area of the fibers, and the ability of sucrose to reduce drug precipitation.[7] Figure 8C indicates that this also appears to be the case for the freshly prepared ITZ-loaded sucrose microfibers, exhibiting up to 8-fold super-

DOI: 10.1021/acs.molpharmaceut.6b01126
Mol. Pharmaceutics 2017, 14, 1666−1680

saturation (C_{max}) relative to the equilibrium solubility of the pure drug and PM.

However, the dissolution performance of the corresponding aged samples was not dramatically reduced after storage, as would typically be expected given the well-recognized arguments that the amorphous state should yield higher dissolution rates and apparent drug solubility than the crystalline equivalent. In the particular case of aged samples containing OLZ and PRX, whereby both components (drug and carrier) recrystallized during storage, dissolution profiles were expected to be similar to the corresponding PMs. However, drug concentration achieved from the aged samples was found to be significantly ($p < 0.05$) supersaturated relative to the equilibrium solubility of the pure drugs and PMs. It is interesting to note that simply mixing OLZ and PRX with sucrose as raw materials also leads to an increase in the dissolution rate and apparent drug solubility. This was investigated in our previous work and explained as potential formation of 1:1 stoichiometric water-soluble complexes between both drugs and sucrose.[7]

As shown in Figure 8A,B, OLZ and PRX reached a slightly lower drug concentration ($p < 0.05$) in the first 5 h compared to the equivalent freshly prepared samples. However, differences in the level of drug supersaturation between aged and freshly prepared samples become insignificant ($p > 0.05$) after this time point (after 5 h), reaching the same level of drug concentration: 0.17 mg/mL for OLZ (2.43-fold compared to the pure drug) and 0.12 mg/mL for PRX (2-fold compared to the pure drug). The initial difference may be linked to the recrystallization of the two drugs upon storage, thereby decreasing the driver of supersaturation for both recrystallized drugs. However, the overall enhancement in the apparent solubility for OLZ and PRX from the recrystallized systems compared to the pure drugs and PMs is somewhat unexpected as drug recrystallization will be expected to negate any solubility advantage.

A different relationship between profiles was seen for ITZ systems. Both freshly prepared and aged samples display similar dissolution profiles in that a rapid release was seen up to a high C_{max}, with the ITZ concentration thereafter decreasing probably due to drug recrystallization and precipitation in the dissolution medium, after which a high plateau concentration is seen. However, a significantly higher maximum level of ITZ supersaturation for the aged samples (up to 10-fold compared to the PM) compared to the fresh ones (up to 8-fold compared to the PM) can be clearly seen from the dissolution profiles ($p < 0.05$), along with a higher C_{max} value (71.58 ± 8.2 μg/mL for the aged samples and 56.78 ± 5.9 μg/mL for the fresh samples).

It is worth noting that dissolution profiles of all freshly aged formulations and their corresponding samples after 8 months of storage did not show any significant difference ($p > 0.05$). This agrees well with the solid-state characterization data, whereby the physical state, morphology, and size of all samples stored for 1 day did not show any changes over 8 months of storage at 75% RH/25 °C. This has positive implications for the development of a stable products using this technology.

Overall, the profiles show that formulation into fibers enhances the dissolution profiles of all three drugs; however a further set of observations relates to the effect of recrystallization of the drug and sucrose (PRX, OLZ) or the sucrose alone (ITZ), whereby in all three cases the expected detrimental effect on dissolution does not appear to occur. For the PRX and OLZ, not only the rate of dissolution but the plateau concentration is very largely maintained following recrystallization, the latter indicating inhibition of precipitation following rapid dissolution. In the case of ITZ, the dissolution from the physical mixes is indistinguishable from the drug alone; however, the ITZ kinetic solubility from the fibers is actually enhanced following sucrose recrystallization compared to the fully amorphous freshly prepared systems. There may be several factors involved in this observation. Table 4 shows that the rate of drug dissolution from the recrystallized system is actually initially slower than that of the freshly prepared material, yet a higher C_{max} is obtained; this may be associated with the higher rate of supersaturation build-up, leading to faster nucleation and crystallization in solution.[43,44] Therefore, the initial slower dissolution rate of the recrystallized sucrose matrix in the aged samples may have prevented rapid nucleation, leading to a greater degree of supersaturation.

Table 4. Comparison of ITZ Concentration in Solution from the Dissolution−Supersaturation Profiles Obtained in the First Hour under Nonsink Conditions between Freshly Prepared Samples and 8-Month Aged Samples under 75% RH/25 °C[a]

	ITZ concentration in solution (μg/mL)	
time (min)	freshly prepared microfibers mean ± SD	8-month aged microfibers mean ± SD
3	6.06 ± 0.18	1.81 ± 0.23
5	11.15 ± 0.43	3.75 ± 0.35
10	22.13 ± 2.25	13.77 ± 3.25
15	42.24 ± 7.90	46.38 ± 1.23
30	**56.78 ± 5.91**	62.69 ± 4.15
60	56.67 ± 4.12	**71.58 ± 8.22**

[a]All the ITZ concentration values reported at the same time are statistically different ($p < 0.05$), except for values reported at 15 min. Bold values indicate C_{max}.

It is also worth re-exploring the traditional mechanistic approaches to solid dispersion technology that were suggested for monolithic systems.[45] One possibility for the enhanced dissolution in all three cases lies with the reduction in drug particle size, even in the recrystallized systems, while the intimate proximity of the sucrose may enhance the wetting of the drugs and reduce aggregation during dissolution. A further explanation, which would be in keeping with observed supersaturation effects, is the suggestion of high local concentrations of the sucrose during the dissolution process itself resulting in enhanced solubility of the drug in the dissolving fluid, even if the sucrose in the totality of the dissolution vessel might not be expected to significantly enhance the dissolution rate. Notwithstanding the mechanism involved, the study suggests that it is possible to generate a physical form of the dispersion, which is stable in itself due to prior recrystallization but may also lead to significant dissolution and potentially processing advantages compared to the amorphous fibrous form.

4. CONCLUSION

Temperature-controlled centrifugal spinning is a promising approach for a large scale manufacture of fully amorphous sucrose-based solid dispersions with enhanced dissolution performance for BCS Class II drugs. However, given the hygroscopic nature of the microfibers formed, in this study, we

DOI: 10.1021/acs.molpharmaceut.6b01126
Mol. Pharmaceutics 2017, 14, 1666−1680

principally focused on the potential effect of high humidity conditions (75% RH/25 °C) on microfiber size, morphology, drug distribution, drug physical state, and dissolution performance of freshly prepared microfiber formulations. In particular, the exposure of microfibers to high relative humidity conditions was expected to have a detrimental effect on the physical stability of the final formulations, with a decrease in the dissolution performance being expected over time. In contrast, although significant changes in the fiber morphology and physical state occurred rapidly after exposing freshly prepared amorphous microfibers to a high moisture environment (75% RH), the resultant product's physical stability and drug dissolution performance showed unexpected findings. The early moisture-induced recrystallization of drug-loaded sucrose microfibers under 75% RH changes the appearance of samples from a fiber morphology to a powder, whereby the drug was found to be fairly uniformly distributed. While PRX and OLZ recrystallized along with the carrier, ATR-FTIR and SS-NMR showed that ITZ remained in the amorphous state for the duration of the stability test (8 months). Furthermore, we observed that the apparent solubility for recrystallized OLZ and PRX from the aged samples was supersaturated compared to the drug alone and the PMs.

Taken together, the results from this set of experiments highlight that drugs in microfibrous solid dispersions may not necessarily need to be present in the amorphous state for promoting drug dissolution performance. A range of other factors, including reduction in drug particle size, wetting effects, solubilization in the immediate proximity of the dissolving surface, and inhibition of crystallization, may all play a role.

It is also typically assumed that amorphous materials are difficult to handle and to process into a conventional dosage form that can be manufactured at large scale. Therefore, another important implication of our findings is that it may be possible to develop a microfiber-based formulation with improved performance reasonably easily by using the centrifugal spinning process: fully amorphous drug-loaded microfibers can be easily produced and, if required, immediately recrystallized under controlled temperature and humidity conditions, leaving a product that may overcome the issues of amorphous material stability while retaining the advantage of rapid dissolution.

AUTHOR INFORMATION

Corresponding Author

*Tel: +44 (0) 207 753 5819. Fax: +44 (0) 207 753 5560. E-mail: duncan.craig@ucl.ac.uk.

ORCID

Susan A. Barker: 0000-0003-4880-0253

Duncan Q. M. Craig: 0000-0003-1294-8993

Present Address

⊥Bahijja T. Raimi-Abraham, Institute of Pharmaceutical Science, Department of Pharmacy & Forensic Science, King's College London, Franklin-Wilkins Building, 150 Stamford Street, London SE1 9NH.

Notes

The authors declare no competing financial interest.

ACKNOWLEDGMENTS

This work was supported by the Biotechnology and Biological Sciences Research Council (BBSRC) Industrial CASE studentship (BBSRC reference BB/K011731/1) formerly known as 'Collaborative Awards in Science and Engineering' and Colorcon Limited. Dr. Bahijja Tolulope Raimi-Abraham is funded by the Engineering and Physical Sciences Research Council (EPSRC) (EPSRC reference EP/L023059/1). The authors would like to thank Mr. David McCarthy for SEM images and Dr. Asma Buanz for her support with DVS experiments.

ABBREVIATIONS

ACN , acetonitrile; ATR-FTIR , attenuated total reflectance-Fourier transform infrared; BCS , Biopharmaceutics Classification System; Cl , chlorine; C_{max} , maximum drug concentration in solution; CP , cross-polarization; DLE Drug , loading efficiency; DMSO , dimethyl sulfoxide; DVS , dynamic vapor sorption; ESEM-EDS , environmental field scanning electron microscopy-energy dispersive X-ray spectroscopy; ITZ , itraconazole; log *P* , partition coefficient; MAS , magic-angle spinning; MTDSC , modulated temperature differential scanning calorimetry; M_w , molecular weight; NQS , non-quaternary suppression; OLZ , olanzapine; PM , physical mixture; PRX , piroxicam; RH , relative humidity; S , sulfur; SDS , sodium *n*-dodecyl sulfate; SEM , scanning electron microscopy; SSNMR , solid-state ^{13}C NMR spectroscopy; T_{deg} , degradation temperature; T_g , glass transition temperature; T_m , melting temperature; T_{max} , time of maximum drug concentration in solution; TOSS , total suppression of sidebands

REFERENCES

(1) Baghel, S.; Cathcart, H.; O'Reilly, N. J. Polymeric Amorphous Solid Dispersions: A Review of Amorphization, Crystallization, Stabilization, Solid-State Characterization, and Aqueous Solubilization of Biopharmaceutical Classification System Class II Drugs. *J. Pharm. Sci.* **2016**, *105*, 2527.

(2) Leuner, C.; Dressman, J. Improving drug solubility for oral delivery using solid dispersions. *Eur. J. Pharm. Biopharm.* **2000**, *50* (1), 47−60.

(3) Miller, J. M.; Beig, A.; Carr, R. A.; Spence, J. K.; Dahan, A. A win−win solution in oral delivery of lipophilic drugs: supersaturation via amorphous solid dispersions increases apparent solubility without sacrifice of intestinal membrane permeability. *Mol. Pharmaceutics* **2012**, *9* (7), 2009−2016.

(4) Wlodarski, K.; Sawicki, W.; Haber, K.; Knapik, J.; Wojnarowska, Z.; Paluch, M.; Lepek, P.; Hawelek, L.; Tajber, L. Physicochemical properties of tadalafil solid dispersions−Impact of polymer on the apparent solubility and dissolution rate of tadalafil. *Eur. J. Pharm. Biopharm.* **2015**, *94*, 106−115.

(5) Fernandez-Ronco, M. P.; Salvalaglio, M.; Kluge, J.; Mazzotti, M. Study of the preparation of amorphous itraconazole formulations. *Cryst. Growth Des.* **2015**, *15* (6), 2686−2694.

(6) Serajuddin, A. T. M. Solid dispersion of poorly water-soluble drugs: Early promises, subsequent problems, and recent breakthroughs. *J. Pharm. Sci.* **1999**, *88* (10), 1058−1066.

(7) Marano, S.; Barker, S. A.; Raimi-Abraham, B. T.; Missaghi, S.; Rajabi-Siahboomi, A.; Craig, D. Q. M. Development of micro-fibrous solid dispersions of poorly water-soluble drugs in sucrose using temperature-controlled centrifugal spinning. *Eur. J. Pharm. Biopharm.* **2016**, *103*, 84−94.

(8) Alonzo, D. E.; Zhang, G. G.; Zhou, D.; Gao, Y.; Taylor, L. S. Understanding the behavior of amorphous pharmaceutical systems during dissolution. *Pharm. Res.* **2010**, *27* (4), 608−618.

(9) Yu, L. Amorphous pharmaceutical solids: preparation, characterization and stabilization. *Adv. Drug Delivery Rev.* **2001**, *48* (1), 27−42.

(10) Qian, F.; Huang, J.; Hussain, M. A. Drug−polymer solubility and miscibility: Stability consideration and practical challenges in

DOI: 10.1021/acs.molpharmaceut.6b01126
Mol. Pharmaceutics 2017, 14, 1666−1680

amorphous solid dispersion development. *J. Pharm. Sci.* **2010**, *99* (7), 2941−2947.
(11) Liu, X.; Lu, M.; Guo, Z.; Huang, L.; Feng, X.; Wu, C. Improving the chemical stability of amorphous solid dispersion with cocrystal technique by hot melt extrusion. *Pharm. Res.* **2012**, *29* (3), 806−817.
(12) Save, T.; Venkitachalam, P. Studies on solid dispersions of nifedipine. *Drug Dev. Ind. Pharm.* **1992**, *18* (15), 1663−1679.
(13) Verheyen, S.; Blaton, N.; Kinget, R.; Van den Mooter, G. Mechanism of increased dissolution of diazepam and temazepam from polyethylene glycol 6000 solid dispersions. *Int. J. Pharm.* **2002**, *249* (1), 45−58.
(14) Pina, M. F.; Zhao, M.; Pinto, J. F.; Sousa, J. J.; Craig, D. Q. The Influence of Drug Physical State on the Dissolution Enhancement of Solid Dispersions Prepared Via Hot-Melt Extrusion: A Case Study Using Olanzapine. *J. Pharm. Sci.* **2014**, *103* (4), 1214−1223.
(15) Andrews, G. P.; AbuDiak, O. A.; Jones, D. S. Physicochemical characterization of hot melt extruded bicalutamide−polyvinylpyrrolidone solid dispersions. *J. Pharm. Sci.* **2010**, *99* (3), 1322−1335.
(16) Hancock, B. C.; Parks, M. What is the true solubility advantage for amorphous pharmaceuticals? *Pharm. Res.* **2000**, *17* (4), 397−404.
(17) Chan, S.-Y.; Toh, S.-M.; Khan, N. H.; Chung, Y.-Y.; Cheah, X.-Z. The improved dissolution performance of a post processing treated spray-dried crystalline solid dispersion of poorly soluble drugs. *Drug Dev. Ind. Pharm.* **2016**, *42*, 1800−1812.
(18) Bruce, C.; Fegely, K. A.; Rajabi-Siahboomi, A. R.; McGinity, J. W. Crystal growth formation in melt extrudates. *Int. J. Pharm.* **2007**, *341* (1), 162−172.
(19) Jijun, F.; Lishuang, X.; Xiaoguang, T.; Min, S.; Mingming, Z.; Haibing, H.; Xing, T. The inhibition effect of high storage temperature on the recrystallization rate during dissolution of nimodipine−Kollidon VA64 solid dispersions (NM−SD) prepared by hot-melt extrusion. *J. Pharm. Sci.* **2011**, *100* (5), 1643−1647.
(20) Jørgensen, A. C.; Torstenson, A. S. Humid storage conditions increase the dissolution rate of diazepam from solid dispersions prepared by melt agglomeration. *Pharm. Dev. Technol.* **2008**, *13* (3), 187−195.
(21) Rodríguez-hornedo, N.; Murphy, D. Significance of controlling crystallization mechanisms and kinetics in pharmaceutical systems. *J. Pharm. Sci.* **1999**, *88* (7), 651−660.
(22) Ahlneck, C.; Zografi, G. The molecular basis of moisture effects on the physical and chemical stability of drugs in the solid state. *Int. J. Pharm.* **1990**, *62* (2), 87−95.
(23) Ilevbare, G. A.; Liu, H.; Edgar, K. J.; Taylor, L. S. Understanding Polymer Properties Important for Crystal Growth Inhibition—Impact of Chemically Diverse Polymers on Solution Crystal Growth of Ritonavir. *Cryst. Growth Des.* **2012**, *12* (6), 3133−3143.
(24) Vivek, K.; Reddy, H.; Murthy, R. S. Investigations of the effect of the lipid matrix on drug entrapment, in vitro release, and physical stability of olanzapine-loaded solid lipid nanoparticles. *AAPS PharmSciTech* **2007**, *8* (4), 16−24.
(25) Patel, H.; ten Berge, W.; Cronin, M. T. Quantitative structure−activity relationships (QSARs) for the prediction of skin permeation of exogenous chemicals. *Chemosphere* **2002**, *48* (6), 603−613.
(26) Rhee, Y.-S.; Park, C.-W.; Nam, T.-Y.; Shin, Y.-S.; Chi, S.-C.; Park, E.-S. Formulation of parenteral microemulsion containing itraconazole. *Arch. Pharmacal Res.* **2007**, *30* (1), 114−123.
(27) Barandiaran, J.; Colmenero, J. Continuous cooling approximation for the formation of a glass. *J. Non-Cryst. Solids* **1981**, *46* (3), 277−287.
(28) Baird, J. A.; Van Eerdenbrugh, B.; Taylor, L. S. A classification system to assess the crystallization tendency of organic molecules from undercooled melts. *J. Pharm. Sci.* **2010**, *99* (9), 3787−3806.
(29) Labuza, T. P.; Labuza, P. S. Influence of temperature and relative humidity on the physical states of cotton candy. *J. Food Process. Preserv.* **2004**, *28* (4), 274−287.
(30) Hancock, B. C.; Shamblin, S. L.; Zografi, G. Molecular mobility of amorphous pharmaceutical solids below their glass transition temperatures. *Pharm. Res.* **1995**, *12* (6), 799−806.
(31) Kawakami, K.; Usui, T.; Hattori, M. Understanding the Glass-Forming Ability of Active Pharmaceutical Ingredients for Designing Supersaturating Dosage Forms. *J. Pharm. Sci.* **2012**, *101* (9), 3239−3248.
(32) Marie, S.; Piggott, J. R. *Handbook of Sweeteners*; Springer Science & Business Media, 2013.
(33) Starzak, M.; Mathlouthi, M. Water activity in concentrated sucrose solutions and its consequences for the availability of water in the film of syrup surrounding the sugar crystal. *Zuckerindustrie* **2002**, *127* (3), 175−185.
(34) Hartel, R. W.; Shastry, A. V. Sugar crystallization in food products. *Crit. Rev. Food Sci. Nutr.* **1991**, *30* (1), 49−112.
(35) Mullin, J. W. *Crystallization*; Butterworth-Heinemann, 2001.
(36) Goldstein, J.; Newbury, D. E.; Echlin, P.; Joy, D. C.; Romig, A. D., Jr; Lyman, C. E.; Fiori, C.; Lifshin, E. *Scanning Electron Microscopy and X-ray Microanalysis: a Text for Biologists, Materials Scientists, and Geologists*; Springer Science & Business Media, 2012.
(37) Wassilkowska, A.; Czaplicka-Kotas, A.; Zielina, M.; Bielski, A. An analysis of the elemental composition of micro-samples using EDS technique. *Czasopismo Techniczne* **2015**, *2014*, 133−148.
(38) Kawakami, K.; Miyoshi, K.; Tamura, N.; Yamaguchi, T.; Ida, Y. Crystallization of sucrose glass under ambient conditions: Evaluation of crystallization rate and unusual melting behavior of resultant crystals. *J. Pharm. Sci.* **2006**, *95* (6), 1354−1363.
(39) Mei, Q. S.; Lu, K. Melting and superheating of crystalline solids: From bulk to nanocrystals. *Prog. Mater. Sci.* **2007**, *52* (8), 1175−1262.
(40) Ayala, A. P.; Siesler, H.; Boese, R.; Hoffmann, G.; Polla, G.; Vega, D. Solid state characterization of olanzapine polymorphs using vibrational spectroscopy. *Int. J. Pharm.* **2006**, *326* (1), 69−79.
(41) Reutzel-Edens, S. M.; Bush, J. K.; Magee, P. A.; Stephenson, G. A.; Byrn, S. R. Anhydrates and hydrates of olanzapine: crystallization, solid-state characterization, and structural relationships. *Cryst. Growth Des.* **2003**, *3* (6), 897−907.
(42) Cavallari, C.; Fini, A.; Pérez Artacho-Santos, B. Thermal study of anhydrous and hydrated forms of olanzapine. *Pharm. Anal. Acta* **2013**, *4* (237), 2.
(43) Sun, D. D.; Lee, P. I. Evolution of supersaturation of amorphous pharmaceuticals: the effect of rate of supersaturation generation. *Mol. Pharmaceutics* **2013**, *10* (11), 4330−4346.
(44) Sun, D. D.; Lee, P. I. Evolution of supersaturation of amorphous pharmaceuticals: nonlinear rate of supersaturation generation regulated by matrix diffusion. *Mol. Pharmaceutics* **2015**, *12* (4), 1203−1215.
(45) Craig, D. Q. The mechanisms of drug release from solid dispersions in water-soluble polymers. *Int. J. Pharm.* **2002**, *231* (2), 131−144.

DOI: 10.1021/acs.molpharmaceut.6b01126
Mol. Pharmaceutics 2017, 14, 1666−1680